

# MIMO CHANNEL CAPACITY BASED ON MEASUREMENT RESULTS

Martin Steinbauer<sup>1</sup>, Andreas F. Molisch<sup>1,2</sup>, Alister Burr<sup>2,3</sup>, and Reiner Thomä<sup>4</sup>

<sup>1</sup>Institut für Nachrichtentechnik und Hochfrequenztechnik, Technische Universität Wien  
 Gußhausstraße 25/389, A-1040 Vienna, Austria, email: martin.steinbauer@nt.tuwien.ac.at

<sup>2</sup>FTW Forschungszentrum Telekommunikation Wien, email: Andreas.Molisch@tuwien.ac.at

<sup>3</sup>University of York, York, United Kingdom, email: alister@ohm.york.ac.uk

<sup>4</sup>Technische Universität Ilmenau, Ilmenau, Germany, email: reiner.thomae@e-technik.tu-ilmenau.de

*Abstract*— We investigate the capacity of multiple-input - multiple-output wireless systems in realistic mobile radio channels. A new method for determination of the cumulative distribution function of the capacity is proposed that requires only a single (double-directional) channel snapshot. First, we extract from one measurement run the directions of arrival and directions of departure. We then derive from these a whole ensemble of channel realizations by introducing random phase factors in the multipath components. We exemplify this procedure by measurement data we obtained in microcellular environments. Not only the correlation of the fading between the antenna elements, but also the nonuniform distribution of the powers in the components are major factors limiting the capacity.

## I. INTRODUCTION

In the past three years interest in so-called multiple-input-multiple-output (MIMO) systems, i.e. systems with antenna arrays at both transmitter and receiver, has exploded. In 1998, the now-classical paper by Foschini and Gans [1] showed that such systems have a channel capacity that increases linearly with the number of antennas, assuming that there is an equal number of antennas at transmitter (TX) and receiver (RX). This spurred a wealth of activities in the field. Tarokh et al. [2] developed the fundamentals of space-time codes that can come close to realizing the channel capacity. Other groups investigated the application of OFDM to MIMO systems [3], [4], [5], [6].

In all of these investigations, the model for the mobile radio channel played a key role. For many years, it had been believed that mobile radio channels with a high degree of multipath scattering are hostile and inherently “bad” channels. However, a rich multipath environment is the best possible for MIMO systems. In most of the existing investigations, it was assumed that the fading at all antenna elements at TX and RX was completely decorrelated. Driessen and Foschini [7] have discussed various physical conditions for this condition to hold, and how the capacity changes if this is not fulfilled. Refs. [8], [6], have assumed local scattering around the mobile station, with a rather small angular spread as seen from the base station [9], [10].

This assumption is often fulfilled for macrocells, but not for micro- and picocells.

While most MIMO capacity evaluations are based on a specific model, very little is known about capacity evaluations based on measurement campaigns. One reason for this is certainly the rareness of suitable measurement data. In this paper, we propose a new procedure that allows one to evaluate the cumulative distribution function (cdf) of the capacity from a single MIMO channel snapshot.

The paper is organized as follows: In section II we start out by describing the measurement apparatus and procedure for obtaining the raw data as well as the measured environments. The extraction of multipath parameters and our method for generating capacity cdfs thereupon is given in section III. Section IV is devoted to the interpretation of the obtained capacity results and finally Section V draws some conclusions.

## II. MEASUREMENTS

### A. Measurement procedure

For the measurements, we used the wideband vector channel sounder RUSK ATM [11] in conjunction with a virtual array at the transmitter. The sounder operates at a frequency of 5.2GHz, corresponding to the HIPERLAN band; the measurement bandwidth is 120MHz. At the receiver, a uniform linear array (ULA) is connected via a fast RF switch to the sounder input. The number of antenna elements is 8, with one dummy element at each end. The elements cover a sector of approximately 120°. At the transmitter, a monopole antenna was mounted on a X-Y- positioning device, whose exact locations were in turn controlled by the sounder via a serial RS232 interface. Figure 1 shows the measurement setup.

The data were captured by a two-sided multiplexing technique [12]. For each transmitter position, a burst of 256 snapshots comprising 8 transfer functions (one for each different antenna element) was collected. In order to eliminate all possible time variance, the contributions with zero Doppler frequency were extracted.

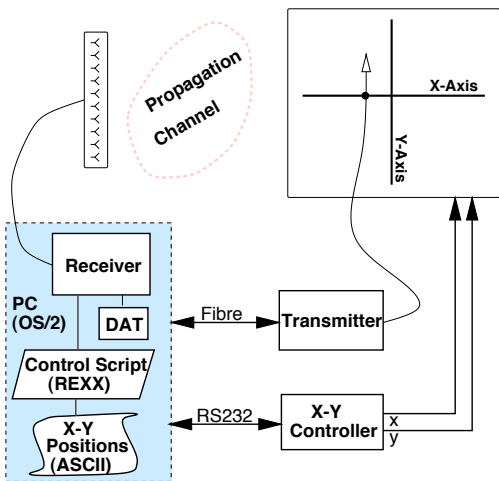


Fig. 1. Measurement setup using an array cross-multiplexing technique.

### B. Environments

The environments investigated were courtyards at the TU Ilmenau in Germany. Transmitter and receiver were both situated in the yard, the RX at the border, the TX more-or-less in the center, depending on the scenario, both at a height of about 1-1.5m, so that the environment can be classified as microcellular. Two of the scenarios were line-of-sight scenarios. In scenario I (a yard open on one side), local scattering very close to the transmitter led to three resolvable quasi-LOS components with identical delay but different directions-of-departure, while in scenario II, only one true LOS component, more than 15dB stronger than any other component, occurred. Scenario III used the same positions of TX and RX as scenario II, but with an obstructed LOS component. Finally, scenario IV was also an obstructed LOS situation in the same (closed) courtyard as scenarios II and III, but with a different receiver position. For scenarios II and III the situation is depicted in Fig. 2. Due to the limited field-of-view of the RX antenna elements, directions of arrival could occur only in a 120° sector. The fact is, however, well taken care of by positioning the RX array in the corner of the yard with broadside to the center.

## III. CAPACITY COMPUTATION

### A. Extraction of multipath parameters

From the raw data, we extracted the directions-of-arrival (DOAs), directions-of-departure (DODs), and delays of the multipath components by nested application of Unitary ESPRIT [13], a parametric subspace estimation method. First, we estimate the delays of the multipath components from the transfer function. The model order, i.e. the number of resolvable com-

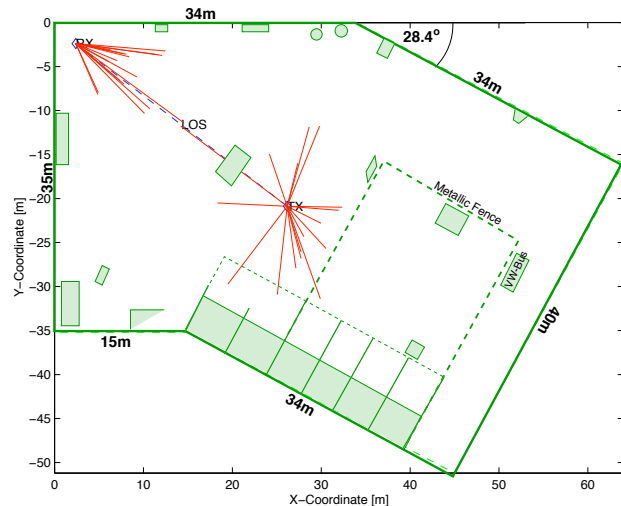


Fig. 2. Closed courtyard of scenarios II-IV with directions-of-arrival and -departure superimposed for scenario III.

ponents, is determined from the relative decrease between neighboring eigenvalues, augmented by visual inspection of the eigenvalue plot. For each of those delay components, we recover the transfer coefficients (between all pairs of antenna elements) by (LS) beamforming with the pseudo-inverse. These in turn are fed into the ESPRIT algorithm again, and allow to estimate the DOAs specifically for each delay. We then again perform beamforming, and feed the results into ESPRIT for the determination of corresponding DODs. In our experiments, the total number of resolvable multipath components (resolvable means resolvable in any domain), was between 14 and 54.

### B. Random phase factors

The above procedure gives the DOAs, DODs, and (complex) amplitudes of the multipath components. We can now obtain different realizations of the channel by simply ascribing a random phase to each multipath component chosen from a uniform distribution. Of course, this phase is independent for the multipath components, but completely correlated for all antenna elements. The phase shifts *between* antenna elements are given by the DOAs and DODs, respectively. For the uniform linear arrays we used, the phase shift is simply  $kd \sin(\varphi_R)$ , or  $kd \sin(\varphi_T)$ , with  $k$  denoting the wavenumber,  $d$  the inter-element distance, and  $\varphi_R, \varphi_T$  the DOAs and DODs wrt. array broadside. The transfer coefficients between the antenna elements are obtained by simply adding up the individual MPC array responses. Repeating the procedure with different phases for the multipath components gives an ensemble of channel realizations. Note that through this summation step we synthesize the narrowband channel response while for the accurate identification of

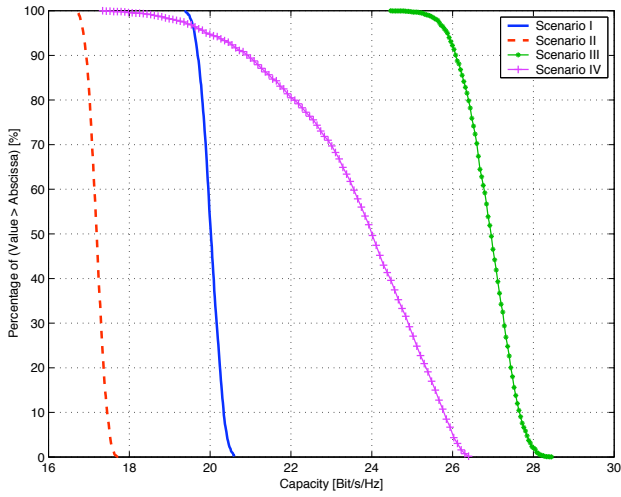


Fig. 3. Complementary cdfs of the MIMO channel capacity encountered in Scenarios I-IV. The SNR is 20dB.

MPCs we used the full wideband data. A cumulative distribution function for the MIMO channel capacity can thus be obtained by applying the capacity formula of Foschini and Gans [1],

$$C = \log_2 \det \left( \mathbf{I} + \frac{\rho}{M_T} \mathbf{H}^H \mathbf{H} \right) \quad (1)$$

to each channel realization. There,  $\mathbf{H}$  denotes the channel transfer matrix,  $\rho$  the SNR, and  $M_T$  the number of TX antennas.  $\mathbf{I}$  is the identity matrix and superscript  $H$  means Hermitian transposition. The normalization is such that the Grammian  $\mathbf{H}^H \mathbf{H}$  is related to the sum of powers of all multipath components.

In comparison to the usual approach, i.e. without the parameter extraction, we can avoid to move transmitter and receiver to different positions and measure the whole set of transfer functions anew at each such position. (Note that although not necessary, this movement could also easily be emulated in our Monte Carlo simulation procedure.)

#### IV. RESULTS AND INTERPRETATION

The extraction and random phase modulation of MPCs (as described above) was applied to measurement data from scenarios I-IV. If not stated otherwise, the following system parameters are envisaged: The MIMO system is made of uniform linear arrays with  $(M_T \times M_R) = (8 \times 8)$  antenna elements; the inter-element spacing is half a wavelength; and the channel SNR is 20dB. For these parameters, Fig. 3 depicts the obtained complementary cdfs for all four scenarios. As can be expected, the cdfs for the line-of-sight scenarios (I-II) are lying leftmost leading to only small capacities in the order of 17-19 bits/s/Hz. Similar values are reported in [14] for a “correlated scenario”

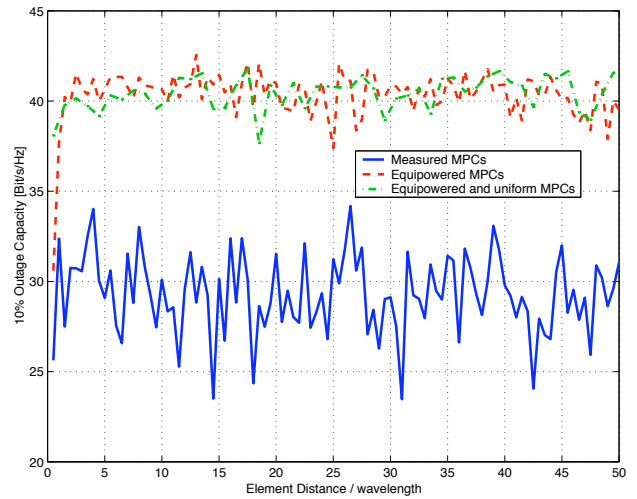


Fig. 4. 10% outage capacity in Scenario III as a function of inter-element spacing. The SNR is 20dB.

but with an  $4 \times 4$  arrangement and 30dB SNR. Fig. 3 corroborates the intuition that the MIMO capacity is highest with many equipowered and decorrelated components. This can be seen from the large capacity in Scenario III where the transmitter is actually in the center of the yard, while in Scenario IV (which is also obstructed LOS) it is near the border restricting relevant multipath to a narrower angular region. Another observation is on the slope of the cdfs. Obviously, the instantaneous capacity in Scenario IV depends much more on the actual fading situation than in the other scenarios. Weaker “channel states” do occur more often reducing the diversity effect, which in turn can again be understood from the reduced angular spread at TX.

From various cdfs we extracted capacities at 10% outage level. These are considered in the sequel in dependence of other parameters.

Looking again on Fig. 3, there is a remarkable increase in the outage capacity ( $\approx 9$  bit/s/Hz at 20dB) just by switching from the LOS to the OLOS case for the centered TX position (Scenario II versus III). This is evidence of the beneficial effect of multipath richness and spreading on the achievable capacity. However, 26 bit/s/Hz is still far below about 40 bit/s/Hz as derived in [1] for independent Rayleigh fading paths.

The dependency of the capacity on the inter-element spacing is shown in Fig. 4 for Scenario III.

Plotted are the outage capacity (solid line) of the channel with the measured multipath parameters (amplitudes, DOAs and DODs), the outage capacities of the same channel with equipowered MPCs (dashed), and that for equipowered MPCs with additional uniform distribution of DOAs and DODs (dash-dotted). The measured outage capacity shows no significant

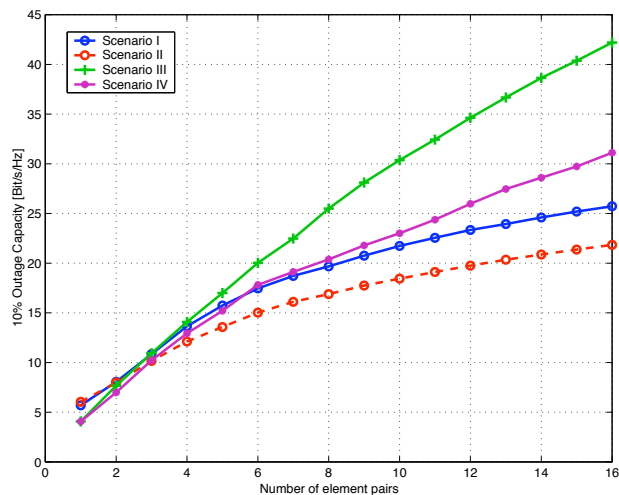


Fig. 5. Outage capacity at 10% level in Scenarios I-IV over the number of antenna element pairs.

increase over the inter-element spacing above  $\lambda/2$ . A similar observation is made in [15] for the case of spatially uniformly distributed scatterers between transmitter and receiver. This indicates that the latter scatterer distribution approximates the microcellular situation best.

For the equipowered MPCs (there are about 37 detected MPCs in this scenario) the outage capacity saturates at about 41 bits/s/Hz as soon as the spacing exceeds one wavelength  $\lambda$ . This is also the maximum value obtained for all spacings when DOAs and DODs are uniformly distributed. The latter corresponds well with the results reported by Foschini and Gans in [1] for statistically independent Rayleigh fading paths.

Figure 5 reports the effect on the capacity when increasing the number of antenna elements at both link ends ( $M_T = M_R$ ).

It can be seen clearly that the capacity gain per additional antenna element is much larger for the OLOS than for the LOS case, a result that is inline with the reasoning of Ref. [7].

## V. CONCLUSIONS

We have proposed a new method for the evaluation of outage capacity in MIMO systems from a single measurement. From double-array measurement data, the DOAs, DODs, and amplitudes of the MPCs are extracted. Using random phases for the MPCs, ensembles of transfer functions and thus cdfs of the capacity can be obtained. We then confirmed our approach by analyzing measurement data in microrcells.

## ACKNOWLEDGEMENTS

We thank Prof. Ernst Bonek for his support and encouragement. Provision of the channel sounder RUSK

ATM by MEDAV GmbH. for performing the measurements is gratefully acknowledged.

## REFERENCES

- [1] G. Foschini and M. Gans, "On limits of wireless communications in a fading environment when using multiple antennas," *Wireless Personal Communications*, vol. 6, pp. 311-335, 1998.
- [2] V. Tarokh, N. Seshadri, and A. Calderbank, "Space-time codes for high data rate wireless communication: Performance criterion and code construction," *IEEE Trans. on Information Theory*, vol. IT-44, pp. 744-765, March 1998.
- [3] Y. G. Li, J. C. Chuang, and N. R. Sollenberger, "Transmitter diversity for OFDM systems and its impact on high-rate data wireless networks," *Journal on Selected Areas in Communications*, vol. SAC-17, p. 1233 ff., July 1999.
- [4] Y. G. Li and N. R. Sollenberger, "Adaptive antenna arrays for OFDM systems with cochannel interference," *Trans. on Communications*, vol. 47, Feb 1999.
- [5] D. Agrawal, V. Tarokh, A. Naguib, and N. Seshadri, "Space-time coded OFDM for high data rate wireless communication over wideband channels," in *Proc. of IEEE Vehicular Technology Conference 1998 (VTC'98)*, pp. 2232-2236, May 1998.
- [6] H. Bölcskei, D. Gesbert, and A. J. Paulraj, "On the capacity of wireless systems employing OFDM-based spatial multiplexing," *submitted to IEEE Trans. on Communications*, Oct 1999.
- [7] P. Driessen and G. Foschini, "Deploying multiple transmit antennas to greatly enhance capacity in wireless channels," *IEEE Transactions on Communications*, vol. COM-47, pp. 173-6, Feb 1999.
- [8] D. Shiu, G. Foschini, M. Gans, and J. Kahn, "Fading correlation and its effect on the capacity of multi-element antenna systems," *IEEE Transactions on Communications*, vol. 48, pp. 502-13, March 2000.
- [9] W. C. Y. Lee, "Effects on correlation between two mobile radio base-station antennas," *IEEE Trans. Comm.*, vol. 21, pp. 1214-1224, 1973.
- [10] J. Fuhl, A. F. Molisch, and E. Bonek, "A unified channel model for mobile radio systems with smart antennas," in *IEE Proceedings on Radar, Sonar and Navigation - Special Issue on Antenna Array Processing Techniques*, vol. 145, pp. 32-41, Feb 1998.
- [11] R. Thomä, D. Hampicke, A. Richter, G. Sommerkorn, A. Schneider, U. Trautwein, and W. Wirtzner, "Identification of time-variant directional mobile radio channels," *IEEE Trans. on Instrumentation and Measurement*, vol. 49, pp. 357-364, April 2000.
- [12] M. Steinbauer, D. Hampicke, G. Sommerkorn, A. Schneider, A. F. Molisch, R. Thomä, and E. Bonek, "Array measurement of the double-directional mobile radio channel," in *Proc. of IEEE Vehicular Technology Conf. 2000 (VTC'2000) - Spring*, (Tokyo, Japan), May 2000.
- [13] M. Haardt and J. Nosssek, "Unitary ESPRIT: How to obtain increased estimation accuracy with a reduced computational burden," *IEEE Trans. on Signal Processing*, vol. 43, pp. 1232-1242, 1995.
- [14] J.-P. Kermaol, P. Mogensen, S. Jensen, J. B. Andersen, F. Frederiksen, T. Sørensen, and K. Pedersen, "Experimental investigation of multipath richness for multi-element transmit and receive antenna arrays," in *Proc. of IEEE Vehicular Technology Conf. 2000 (VTC'2000) - Spring*, vol. 3, (Tokyo, Japan), pp. 2004-8, May 2000.
- [15] A. G. Burr, "Channel capacity evaluation of multi-element antenna systems using a spatial channel model," in *Proc. of Millennium Conf. on Antennas & Propagation (AP'2000)*, no. #0231 on CD-ROM, (Davos, Switzerland), April 2000.